EFFECT OF SiO_2-Y_2O_3-Al_2O_3 ADDITION ON DENSIFICATION OF SILICON CARBIDE CERAMICS

Marchi, J.; Bressiani, J. C.; Bressiani, A. H. A.

IPEN - Instituto de Pesquisas Energéticas e Nucleares
Travessa R, 400 – Cidade Universitária
CEP: 05508-900 - São Paulo - SP – Brasil
e-mail: jmarchi@net.ipen.br; abressia@net.ipen.br

Key words: silicon carbide, liquid phase sintering, additives

Abstract. In this work, several compositions based on SiO_2-Y_2O_3-Al_2O_3 system were mixed together with 90% volume silicon carbide in order to achieve high density materials. Pressurelless sintering experiments were carried out in a graphite resistance furnace at 1950ºC/1h. The sintering additive performance was evaluated from density and weight loss data. The crystalline phases were identified by x-ray diffraction. Vickers hardness indentations were performed with 70 N load, and the fracture toughness was calculated from indentation geometry and crack length data. The results show that homogeneous silicon carbide ceramics can be obtained, achieving densities higher than 90% of theoretical density. Vickers hardness at about 20 GPa and fracture toughness up to 7 $Mpa.m^{1/2}$ were obtained.

Introduction

Silicon carbide (SiC) is an important structural ceramic applied in a wide range of fields, such as automotive engine components, cutting tools, abrasives, etc. The extensive applications can be possible due to its low density, high hardness, and high mechanical and wear resistances.

Silicon carbide can be sintered with boron and/or carbon additions, through solid state mechanism. In this case, temperatures higher than 2100ºC should be used, and the material present low fracture toughness. Sintering of silicon carbide can also occurs via liquid phase using metallic oxides as additives. The most used additives are alumina, yttria, silica and rare earth oxides [1]. During sintering these oxides form a low viscosity liquid phase and thus promote the densification of silicon carbide ceramics. The knowledge of phases and phases relationships in multi-components systems is of fundamental importance in order to optimize the microstructure and properties of ceramic specimens [2]. This sintering process produces a more homogeneous microstructure that increases the fracture toughness. The sintering temperatures are usually around 1950ºC.

Hardness measurements gives useful information about mechanical properties of ceramic bodies, including stresses field, elastic module, fracture toughness parameters and crack propagation [3]. The silicon carbide hardness depends on densification method, chemical composition, density, grain

orientation and microstructural features, such as grain size, grain morphology and grain boundaries phase [4-5].

The fracture toughness in association with others properties is an important parameter to evaluate ceramic materials for engineering applications. The fracture toughness of brittle materials can be determined by Vickers hardness test. A load is applied with a pyramidal diamond tip, producing an indentation on the ceramic surface. A zone deformation, which can be elastic or plastic crack propagation are observed after relieving the load. The toughness models based on crack development are usually classified in two main systems [6]: halfpenny or Palmqvist. Fig. 1 is an example of crack geometry of both systems around Vickers indentation [7]. The models are being sophisticated after Palmqvist studies, establishing the relations between stress fields and the deformation produced in a material. Some equations [7-8] are used in order to get fracture toughness values closer to the real one. A general equation [9] was developed to be used independent on the crack system.

The crack extension of silicon carbide based ceramics can be influenced by grain morphology, characteristics of the secondary phase present in grain boundaries and silicon carbide phase transformation during densification [10-11].

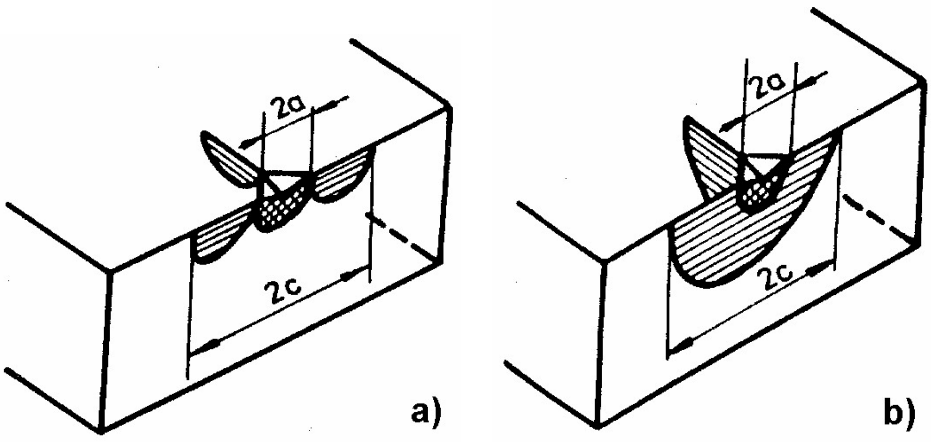

Fig. 1: crack systems around Vickers indentation (a): Palmqvist; (b): half-penny [7]

The aim of this work is to evaluate some compositions in the SiO_2-Y_2O_3-Al_2O_3 system to obtain a high density silicon carbide ceramic with homogeneous microstructure and high mechanical properties.

Experimental Procedure

The raw materials used in this work were silicon carbide (SiC, H. C. Starck, BF-17, 91.9% β), alumina (Al_2O_3, Alcoa, A-16 SG, 99.9%), silica (SiO_2, Fluka) and yttria (H. C. Starck, grade C, 99.99%). Several compositions were prepared according to Table 1. The mixtures of oxides were mechanically homogenized for 4 hours. The final compositions contain 10 mol% of additives and 90 mol% silicon carbide and were milled in attritor for 4 hours. The mixtures were dried in a rotoevaporator and uniaxially pressed at 20 MPa. The samples were then cold isostatically pressed at 200 MPa.

Table 1: Mixture compositions

Composition	*% mol SiO_2*	*% mol Y_2O_3*	*% mol Al_2O_3*	*Y_2O_3:Al_2O_3 ratio*	*additives weight %*
60S-20Y-20A	60	20	20	1:1	11.32
50S-25Y-25A	50	25	25	1:1	11.82
40S-40Y-20A	40	40	20	2:1	12.68
40S-30Y-30A	40	30	30	1:1	12.21
40S-20Y-40A	40	20	40	1:2	11.73
33S-33Y-33A	33.33	33.33	33.33	1:1	12.61
20S-60Y-20A	20	60	20	3:1	15.31
20S-40Y-40A	20	40	40	1:1	14.91
20S-20Y-60A	20	20	60	1:3	12.44

Pressurelless sintering experiments were carried out in a graphite resistance furnace (Astro), using 60S-20Y-20A composition as protective powder bed. Sintering was conducted under argon flow and a heating rate of 15ºC/min was applied up to 1950ºC, keeping this dwell time for 1 hour. The samples were characterized by density measurements using Archimedes method and by weight loss evaluation. The theoretical densities were calculated according to the rule of mixtures.

The polished cross section samples were observed by scanning electron microscopy (SEM). After polishing, the samples were chemically etched with Murakami´s solution in order to reveal the grains morphology. Mechanical properties at room temperature were evaluated by Vickers hardness indentation. The load was varied from 10N up to 100N on the polished cross section of 50S-25Y-25A sample. Ten indentation were performed in each sample, keeping the distance between two indentations centers more than three crack lengths. The Vickers hardness and fracture toughness were calculated from indentation diagonal and crack length data [9].

Results and Discussion

Table 2 presents both green and sintered densities of silicon carbide as well as the weight loss. It can be seen that densities greater than 90% were obtained for all sintered samples. Keeping the Al_2O_3 amount constant in 20 mol%, it can be seen that the density decreases, as the SiO_2 amount increases. The same behavior was observed keeping the Y_2O_3 amount constant in 20 mol % as well as keeping the Y_2O_3/Al_2O_3 ratio constant in 1:1. When the SiO_2 amount was fixed in 40 mol % or in 20 mol %, higher densities was obtained when the Y_2O_3/Al_2O_3 ratio was 1:1. It was observed (Table 2) that higher densities were obtained if lower SiO_2 amount was added. This fact can indicates that the presence of oxygen on the silicon carbide surface powder can be possibly enough to supply SiO_2 to reduce the temperature for the liquid phase formation. The highest density was obtained for 20S-40Y-40A, which achieved 95.77% of theoretical density.

The weight loss did vary from 3.41% to 8.52% and did not present a direct correspondence with densities values. The weight loss is caused by reactions of the additives with silicon carbide. Some of them are shown in Eq. 3 to 6 [12-13] .This problem is well avoided if powder bed is used to cover the samples during sintering. In this work, it could be noticed the efficient of 50-S-25Y-25A powder bed composition to reduce the weight loss. This powder bed creates an equivalent partial pressure of the

volatile specimens, reducing the driving force for diffusion out of the sample [14]. So, it can be responsible for limit the escape of volatile components of the additives from the bulk sample. Even with the use of a mixture powder bed, it can be seen (Table 2) that higher contents of alumina or silica are responsible for the increasing in weight loss, due to volatile products formation according to Eq. 1 to 4.

Table 2: Results of sintering in graphite resistance furnace

Sample	*green density (% td)*	*hydrostatic density (% td)*	*weight loss (%)*
60S-20Y-20A	55.35 ± 0.02	90.37 ± 0.07	7.75 ± 0.04
50S-25Y-25A	54.98 ± 0.02	92.20 ± 0.08	6.78 ± 0.03
40S-40Y-20A	55.21 ± 0.03	93.73 ± 0.08	5.52 ± 0.01
40S-30Y-30A	53.90 ± 0.03	94.13 ± 0.01	8.83 ± 0.42
40S-20Y-40A	54.02 ± 0.01	92.15 ± 0.01	8.52 ± 0.20
33S-33Y-33A	55.28 ± 0.02	95.43 ± 0.03	6.45 ± 0.15
20S-60Y-20A	53.80 ± 0.02	94.80 ± 0.01	3.41 ± 0.08
20S-40Y-40A	54.78 ± 0.03	95.77 ± 0.12	4.60 ± 0.33
20S-20Y-60A	54.35 ± 0.03	95.14 ± 0.04	7.91 ± 0.14

$SiC\ (s) + Al_2O_3\ (s) \rightarrow SiO\ (g) + Al_2O\ (g) + CO\ (g)$ Eq. 1

$2\ SiC\ (s) + Al_2O_3\ (s) \rightarrow Al_2O\ (g) + 2\ Si\ (l) + 2\ CO\ (g)$ Eq. 2

$3\ SiC\ (s) + Al_2O_3\ (s) \rightarrow 2\ Al\ (l) + 3\ Si\ (l) + 3\ CO\ (g)$ Eq. 3

$2\ SiC\ (s) + SiO_2\ (s) \rightarrow 3\ Si\ (l) + 2\ CO\ (g)$ Eq. 4

Fig. 2 represents the x-ray diffraction pattern of silicon carbide samples, sintered at 1950ºC/1h. β and α-SiC are identified as major phases, indicating the incomplete β–α transformation. $Y_2Si_2O_7$ and YAG were identified as secondary crystalline phases, as expected from the SiO_2-Al_2O_3-Y_2O_3 phase diagram [15].

Fig 3a shows the Vickers hardness values as a function of the applied load on the polished cross section of 20S-40Y-40A sample. It can be seen that values greater than 70 N can produce constant values of Vickers hardness. 70 N was the inferior limit acceptable. For this reason, all Vickers hardness tests were performed with a 70 N load. A typical Vickers indentation on the polished cross section sample is shown in Fig. 3b. The results obtained of Vickers Hardness and fracture toughness of some samples are presented in Table 3. It can be noticed that Vickers hardness greater than 20 GPa were obtained for all samples analyzed. Difference in density values promotes a slight variation in Vickers hardness. Values of fracture toughness varied from 6.2 to 7.1 $MPa.m^{1/2}$. Higher values of Vickers hardness were associated with lower values of fracture toughness. Because of the inverse proportion behavior of such variables, in general one property is favored related to another, aimed for specific application.

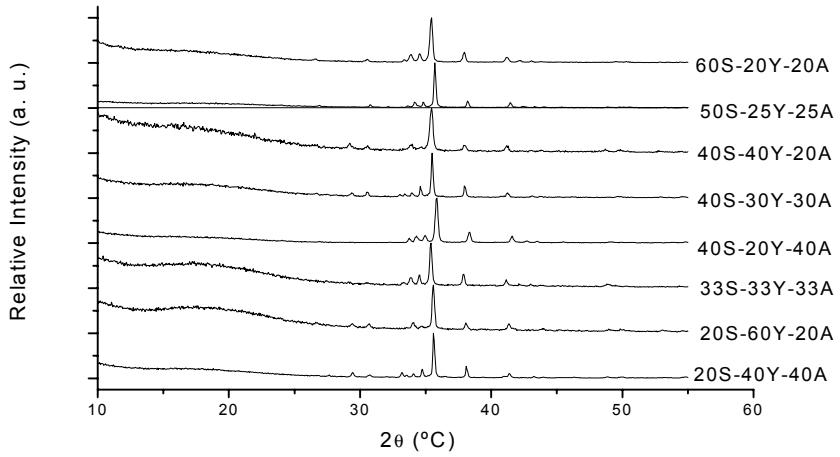

Fig.2: X-ray diffraction pattern of sintered silicon carbide (1950ºC/1h)

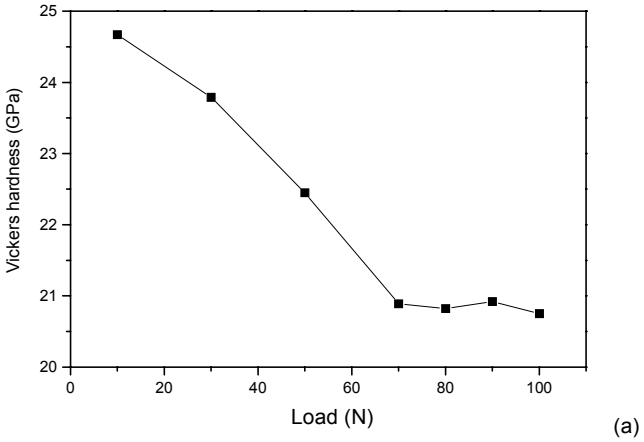

(a)

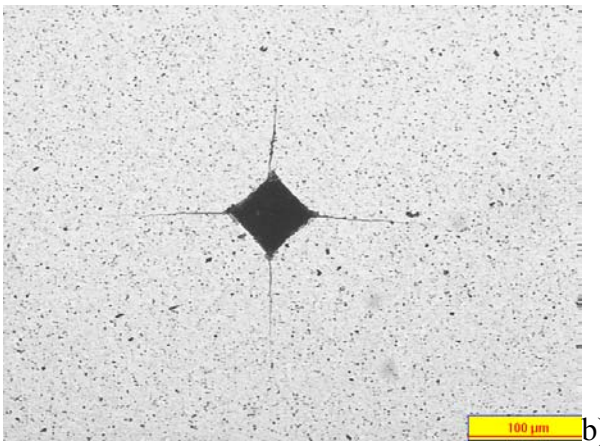

b)

Fig. 3: a) Vickers hardness values as a load function stablished on polished cross section of 20S-40Y-40A sample b) Optical micrograph of Vickers indentation on the 20S-40Y-40A sample

Table 3: Results of mechanical properties

Sample	*Vickers Hardness (GPa)*	*Fracture Toughness (MPa.m$^{1/2}$)*
40S-20Y-40A	20.7 ± 0.7	7.1 ± 0.4
20S-40Y-40A	20.9 ± 0.7	6.2 ± 0.3
20S-20Y-60A	20.8 ± 1.5	6.6 ± 0.3

Fig. 4 shows a typical scanning electron micrographs of sintered sample. It can be seen (Fig. 4a) that the additives are well distributed in the silicon carbide matrix. After Murakami´s etching, the morphology of the silicon carbide grains is revealed (Fig. 4b).

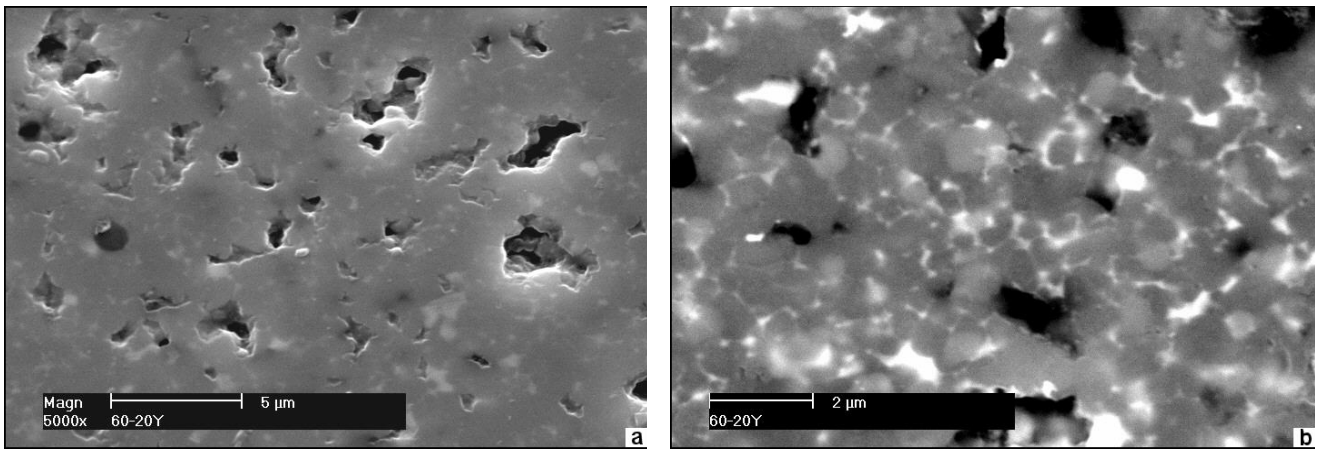

Fig. 4: Scanning electron micrographs of sintered sample 50S-25Y-25A
a) after polishing; b) after Murakami's etching

Conclusions

Suitable compositions in SiO_2-Al_2O_3-Y_2O_3 system are used to sintering silicon carbide, reaching densities up to 95% of theoretical density. The best results were obtained for lower SiO_2 amount (20 mol%) and $1Al_2O_3$: $1Y_2O_3$. β and α SiC are identified in sintered silicon carbide samples, indicating a not complete β–α transformation. 10 vol % of additives, in several proportions, also produce $Y_2Si_2O_7$ and YAG as crystalline secondary phases. Vickers hardness of 20 GPa and fratcture toughness of 7 MPam ½ can be obtained resulted from homogeneous microstructure of the samples.

Acknowledgements

The authors gratefully thanks CNPq, PRONEX and FAPESP for financial support.

References

[1] V. A. Izhevskyi; L. A. Genova; A. H. A. Bressiani; J. C. Bressiani, Key Eng. Mater.173-180 (2001), p. 120-125

[2] U. Kolitsch; H. J. Seifert; F. Aldinger, J. Phase Eq. 19 (1998), p. 426-433
[3] I. J. McColm, Ceramic Hardness; Plenum Press, NY (1990)
[4] S. S. Shinozaki; J. Hangas; K. R. Carduner; M. J. Rokosz, J. Mater. Res. 8 (1993) p. 1635-1643
[5] Y. W. Kim; M. Mitomo; H. Emoto; J. G. Lee, J. Am. Ceram. Soc 81 (1998) p. 3136-3140
[6] C. B. Ponton; R. D. Rawlings, Mater. Sci. and Tech. 5, (1989), p. 865-871
[7] J. Dusza, Scrip. Met. and Mat. 26 (1992), p. 337-342
[8] K. Niihara, J. Mater. Sci. Letters 2 (1983), p. 221-223
[9] K. M. Liang; G. Orange; G. Fantozzi, J. Mater. Sci 25 (1990), p. 207-214
[10] D-H. Kim; C. H. Kim, J. Am. Ceram. Soc 73 (1990) p. 1431-1434
[11] S. K. Lee; C. H. Kim, J. Am. Ceram. Soc 77 (1994) p. 1655-1658
[12] M. A. Mulla; V. D. Krstic, Ceram. Bull. 70 (1991), p. 439-443
[13] V. A. Izhevskyi; L. A. Genova; A. H. A. Bressiani; J. C. Bressiani, Ceramic Mat. and Comp. for Engines, p. 593-598 – Wiley VCH, Weinhein, Ed. Jurgen, G. Heinrich and F. Aldinger, 2001
[14] E. Jennifer Winn; W. J. Clegg, J. Am. Ceram. Soc 82 (1999) p. 3466-3470
[15] A. Bondar; F. Y. Galakhov, In E. M. Levin; C. R. Robbins; H. F. McMurdie, Phase diagrams for Ceramistis, Supplement, p. 107 The American Ceramic Society, 1969